Hartree-Fock-Bogoliubov description of quasiparticle excitations in the superdeformed wells of ^{191,192}Hg and ^{192,193}Tl

P.-H. Heenen
Service de Physique Nucléaire Théorique, U.L.B.-C.P.229, B-1050 Brussels, Belgium

R. V. F. Janssens
Argonne National Laboratory, Argonne, Illinois 60439
(Received 20 August 1997)

The properties of superdeformed bands in ^{191,192}Hg and ^{192,193}Tl have been studied using the cranked Hartree-Fock-Bogoliubov method with the Lipkin-Nogami prescription, the Skm* interaction, and a surface-delta, density-dependent pairing force. In particular, quasiparticle excitations involving intruder orbitals are analyzed in detail. Comparisons between data and calculations are performed for $\mathcal{J}^{(2)}$ moments, quadrupole moments, spins, transition energies, and alignments. [S0556-2813(98)04601-9]

PACS number(s): 21.10.Re, 21.60.Jz, 27.80.+w

I. INTRODUCTION

Superdeformed (SD) rotational bands have by now been established in a number of regions of the periodic table ranging in mass from $A\sim60$ to $A\sim240$. The most extensive sets of data are presently on hand for nuclei near $A\sim150$ and $A\sim190$. In both regions, a large number of nuclei have been shown to exhibit band structures associated with the rotation of a prolate intrinsic state with a major-to-minor axis ratio of roughly 2:1 ($A\sim150$) and 1.6:1 ($A\sim190$). Furthermore, in many of these nuclei, a number of SD bands have been reported; i.e., excitations above the yrast line have been studied in the second well. The rotational frequencies ($\hbar\omega$) and, hence, the angular momenta at which the bands are observed in the two regions are quite different. In ^{152}Dy, the nucleus often regarded as the ''doubly magic'' SD nucleus of the $A\sim150$ region because of the presence of large shell gaps at $Z=66$ and $N=86$ in the single-particle spectrum, the SD bands span transition energies from ~650 to 1500 keV. In contrast, the γ-ray energies observed in ^{192}Hg ($Z=80$, $N=112$) extend from roughly 250 keV to 850 keV. Because of this difference in the frequencies involved, the behavior of the SD bands in the two regions and, in particular, the behavior of the dynamic moment of inertia $\mathcal{J}^{(2)}$, are sensitive to different physical processes. More precisely, the evolution of the $\mathcal{J}^{(2)}$ moment with $\hbar\omega$ has been shown to be particularly sensitive to the occupation of specific high-N intruder orbitals in the $A\sim150$ SD nuclei. The role of these orbitals in the $A\sim190$ region is less prominent because of pairing effects at the lower frequencies involved.

This paper presents a theoretical study of SD bands in ^{192}Hg and surrounding odd-even and odd-odd nuclei. It focuses mainly on the description of bands associated with intruder ($j_{15/2}$ neutron and $i_{13/2}$ proton) quasiparticle excitations. Experimentally, this type of configuration has been assigned to a number of bands in the Hg and Tl isotopes. The $\mathcal{J}^{(2)}$ moments of these bands exhibit noticeable changes from nucleus to nucleus which represent a challenge for theory to understand. The method used here has been presented in Refs. [1,2] and has been shown to reproduce with good accuracy the SD band properties of even nuclei [2,3]. It is based on the cranked Hartree-Fock-Bogoliubov (HFB) approach where the mean-field method is corrected by means of the Lipkin-Nogami prescription [4–6] to restore approximately the correct particle number. The nucleon-nucleon effective interaction used in the particle-hole channel is the Skyrme force within the Skm* parametrization [7–9], and in the pairing channel, a zero-range force with a surface-peaked density dependence [2] is used.

The approach followed hereafter is in many ways similar to that used in experiments: From the results of the calculations, quantities such as the spin, parity, and excitation energy as well as the associated rotational frequencies, the $\mathcal{J}^{(2)}$ moments, and the gain in alignment are extracted for each configuration being investigated. The paper focuses first on the ^{192}Hg nucleus and presents results for the yrast SD band as well as for several low-lying quasiparticle excitations. Subsequently, excitations involving intruder orbitals are probed in the odd-even ^{191}Hg and ^{193}Tl isotopes. Finally, calculations are also presented for the odd-odd nucleus ^{192}Tl.

As stated above, the present work deals with quasiparticle excitations and a word of caution may be on order. From recent random phase approximation (RPA) calculations [10], it has been proposed that most, if not all, of the excited SD bands in even-even nuclei of the $A\sim190$ region correspond to collective, octupole vibrations. This type of excitation is not considered here and will be discussed in a forthcoming publication [11]. Also, methods based on effective interactions cannot be expected to reproduce all the details of experimental results. In particular, level crossings are often too sensitive to the details of the method to be reproduced in a systematic way. This is why the choice is made here to perform comparisons for an extended set of bands with the hope that this approach will give insights into generic features and improve the general understanding of the mechanism(s) leading to excitations in the SD well.

II. QUASIPARTICLE EXCITATIONS IN ^{192}Hg

The calculations discussed hereafter can be regarded as an extension of those presented for the ^{193}Hg and ^{195}Pb nuclei

TABLE I. Excitation energies (in MeV) of various one- and two-quasiparticle (qp) bands, compared with their estimate as derived from the quasiparticle energies in ^{192}Hg. The comparison is performed at $\hbar\omega=0.3$ MeV.

	qp	E^*	$\Delta e_{\rm qp}$
^{191}Hg	7^-	0.	-
	7^+	0.36	0.33
^{192}Hg	[642]3/2 [512]5/2	1.40	1.70
	[642]3/2 7^-	1.10	1.15
	7^+ 7^-	1.20	1.10
^{192}Tl	7^- 6^+	0.0	0.0
	7^- 6^-	0.03	0.04
	7^+ 6^-	0.30	0.33
^{193}Tl	6^-	0.0	-
	6^+	0.04	0.03

in Ref. [9]. Table I summarizes the nuclei and the quasiparticle excitations under discussion.

As mentioned above, the ^{192}Hg nucleus plays a special role for SD nuclei near $A\sim190$. Thus, it is important to confront calculations and experiment for this nucleus, especially if a systematic study of the region is being attempted. Experimentally, besides the yrast SD band, two excited SD bands have been observed in experiments with Gamma sphere [12] and Eurogam [13]. For these two bands, the dynamical moments of inertia exhibit a large peak (''backbend like'') (band 2) or a strong upbend (band 3) at frequencies $\hbar\omega\sim0.3$ MeV. Such pronounced irregularities in $\mathcal{J}^{(2)}$ are not seen in any of the yrast SD bands of the even-even nuclei of the region, with the exception of ^{190}Hg [14]. It is worth noting that the ''critical'' frequency where the rise in $\mathcal{J}^{(2)}$ starts differs slightly for the two bands.

The neutron quasiparticle diagram that had been obtained in Ref. [2] for the ^{192}Hg yrast band is given on the right-hand side of Fig. 1. The quasiparticles are labeled by their dominant Nilsson component in the HF basis and by an index p or h indicating whether this component lies above or below the Fermi level. Such a labeling, although approximate [15], is used as a guide to construct the excited bands. From Fig. 1, it is clear (i) that the energetically most favorable two-quasiparticle excitations are based on one quasiparticle of the particle type and another of the hole type, and (ii) that excitations based on one of the [642]3/2 signature partner orbitals and on either a $N=7$ or a [512]5/2 state are most likely involved in the lowest excitations. These negative parity orbitals exhibit a crossing around $\hbar\omega=0.1$ MeV for both signatures.

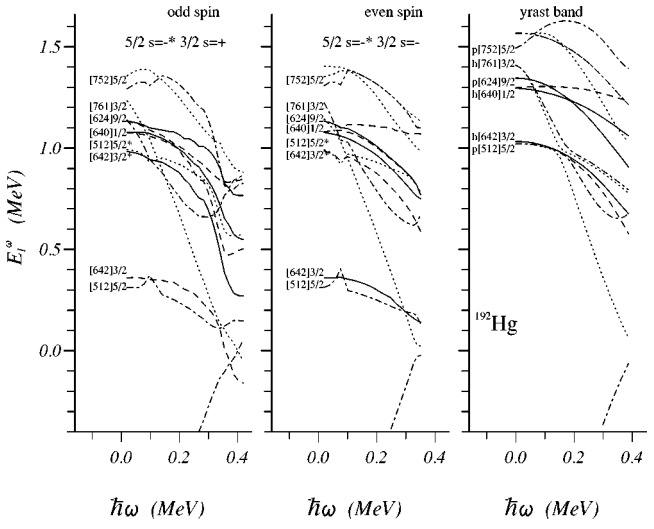

FIG. 1. Neutron quasiparticle Routhians in ^{192}Hg for the yrast band (right-hand panel) and the two-quasiparticle excitations where the $[512]5/2(s=-)$ orbital is coupled to either of the two signatures of the [642]3/2 orbital (middle and left-hand panels).

Generally speaking, the self-consistent creation of quasiparticles modifies the quasiparticle diagram of Fig. 1 significantly. Within the BCS approximation, the energy of the ith quasiparticle is given by $\sqrt{(\epsilon_i-\lambda_\tau)^2+\Delta_i^2}$, and all levels are shifted by a readjustment of the Fermi level λ_τ to recover the right number of particles. A second change is caused by the reduction of the pairing correlations due to the creation of quasiparticles. The pairing matrix elements Δ_i are reduced in a way which depends on the state i. The main consequence of this reduction is a compression of the quasiparticle spectrum. A more subtle effect is related to the breaking of time reversal invariance when the excitation involves a quasiparticle without its signature partner. The time odd terms of the Skyrme functional [16–18] are then different from zero and remove the degeneracy between signature partners. These terms affect the single-particle mean-field energies ϵ_i, and it has been noticed in previous works [3,8,9,19] that the effect is the largest for the signature partners of the quasiparticles which are being created. With current parametrizations of Skyrme forces, their mean-field energies come closer to the Fermi energy and consequently, the energy of the corresponding quasiparticle is lowered.

All these effects are illustrated in the two other panels of Fig. 1, for the case of the creation of two quasiparticles corresponding to the negative signature of the [512]5/2 level coupled to either of the two signatures of the [642]3/2 orbital. The quasiparticle energies given in the figure are those of the vacua determined self-consistently for each two-quasiparticle state. Both spectra are clearly compressed with respect to the calculations for the yrast configuration (right-hand side, Fig. 1), reflecting the decrease of the pairing correlations. However, the ordering of the levels is not modified significantly. The most noticeable difference concerns the signature partners of the quasiparticle excitations: Their energies are reduced by more than 0.5 MeV. The image in the negative sea of the quasiparticles having an energy lower than 500 keV has also been added to Fig. 1. The interactions between quasiparticles are clearly much more complicated than in the case of the ^{192}Hg yrast SD band, leading, for example, to different patterns for the alignment $j_{15/2}$ quasiparticles.

The calculated $\mathcal{J}^{(2)}$ moments are presented as a function of $\hbar\omega$ in the right panel of Fig. 2 for the yrast configuration and most of the two-quasiparticle excitations that have been considered in the present work. The available experimental data are given for comparison (left panel). From this figure, it is clear that the effects discussed above, i.e., the changes in the quasiparticle energies brought about by the creation of quasiparticle excitations, can have a rather dramatic impact

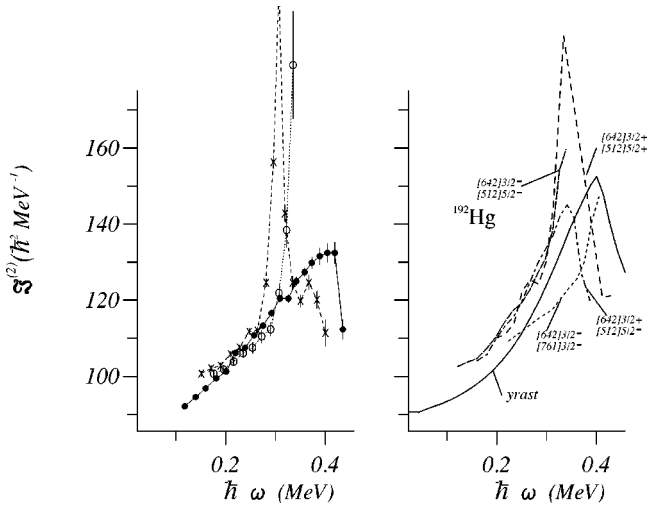

FIG. 2. Comparison between the experimental $\mathcal{J}^{(2)}$ moments of inertia (left panel) for the three SD bands of ^{192}Hg [12] and the moments calculated for the various configurations indicated in the figure (right panel).

on the $\mathcal{J}^{(2)}$ moment: Sharp rises and ''backbend''-like features appear at certain frequencies.

The trend with $\hbar\omega$ of the calculated $\mathcal{J}^{(2)}$ moment for the ^{192}Hg yrast SD band reproduces the general behavior displayed by the data; i.e., there is a smooth rise over most of the range in frequency. The calculations also predict a sudden decrease for $\hbar\omega > 0.38$ MeV. This decrease may also be present in the data, although this observation is based solely on the last data point which has only been assigned tentatively [12]. The present calculated result has already been discussed in Ref. [2] where it was shown that the smooth rise in the $\mathcal{J}^{(2)}$ moment is due to changes in the pairing strength brought about mostly by the gradual alignment of $j_{15/2}$ neutrons. The sudden drop at the highest frequencies occurs when this alignment has been completed.

Table I provides the excitation energies computed for the two-quasiparticle excitations under consideration. For each band, these energies are obtained from the difference between the total energy of the band and the total energy of the lowest SD band of the nucleus. These calculations are performed at a fixed frequency $\hbar\omega = 0.3$ MeV. From this table it is clear that the lowest excitation energy corresponds to a band based on the negative signature of the [761]3/2 orbital coupled to the [642]3/2 orbital. The excitation involving the two signatures of this $N=7$ orbital (7^+7^- in Table I) lies at nearly the same energy, while those involving the [642]3/2 and the [512]5/2 orbitals are located 300 keV higher. The $\mathcal{J}^{(2)}$ moment of inertia of the band associated with the two signatures of the $N=7$ neutron orbital (not shown in Fig. 2) is calculated to be flat as a function of $\hbar\omega$ and is, thus, unlikely to be associated with bands 2 and 3 in ^{192}Hg.

From the right-hand side of Fig. 2 it can be seen that the two-quasiparticle excitation involving the negative signature of the [512]5/2 and the positive signature of the [642]3/2 orbitals exhibits a peak in the $\mathcal{J}^{(2)}$ moment around $\hbar\omega = 0.32$ MeV. In contrast, no such peak is seen for the excitation based on the same [512]5/2 orbital with the negative signature of the [642]3/2 orbital, at least in the range of frequency covered by the experiments ($\hbar\omega \leqslant 0.45$ MeV). However, this difference in behavior is directly related to a small difference in the position of the quasiparticle levels (Fig. 1), which may well be within the uncertainties of the method. Again, this observation illustrates how difficult it is in a nonparametric approach like the one used here to obtain crossings at the right frequencies or even to deduce the behavior of an excited band by simply examining the quasiparticle diagram of the unperturbed vacuum. On the other hand, these excited SD bands probably provide the opportunity to investigate the effect of the time odd terms of Skyrme forces and to improve on their otherwise poorly determined parametrization.

Despite these reservations, it is gratifying to find excitations which result in $\mathcal{J}^{(2)}$ moments displaying variations with frequency resembling closely those seen in the data. For example, the $[512]5/2(s=-)*[642]3/2(s=+)$ configuration and, perhaps, the $[512]5/2(s=+)*[642]3/2(s=+)$ one reproduce the data for band 2, while the $[761]3/2(s=-)*[642]3/2(s=-)$ or the $[512]5/2(s=-)*[642]3/2(s=-)$ configuration exhibit similarities with band 3. We note that the first of these two configurations exhibits a rise in $\mathcal{J}^{(2)}$ starting at higher $\hbar\omega$ than the other, a feature which has similarities with the data. A more definite configuration assignment to either of the known SD bands is, however, impossible at this time as it would require more detailed experimental data, i.e., data points at higher frequencies and/or the discovery of additional bands. More importantly, as the two possible configurations for band 2 result in sequences with odd and even spins, respectively, an experimental determination of these quantum numbers would be very useful.

III. INTRUDER CONFIGURATIONS IN ^{191}Hg, ^{193}Tl, AND ^{192}Tl

Besides the quasiparticle excitation energies, Table I also presents the excitation energies as calculated from the quasiparticle energies of the ^{192}Hg yrast SD band (right panel, Fig. 1). For ^{192}Hg, this energy is equal to the sum of the energies of the quasiparticles created on the ^{192}Hg vacuum. For one-quasiparticle bands, the excitation energy is given by the difference between the energy of the quasiparticle corresponding to a given band and the energy corresponding to the lowest SD band in the same nucleus. The calculations are performed at a rotational frequency of 0.3 MeV. This approach has two main deficiencies. First, it does not take into account any self-consistency effects, in particular the change in particle number and in deformation due to the creation of quasiparticles. Second, it is also an ambiguous procedure, because of the inclusion of correlations beyond a mean-field approach in the Lipkin-Nogami prescription. As discussed in Ref. [1] by Gall *et al.*, the quasiparticle energies are no longer uniquely defined: The $\lambda_2\langle\Delta\hat{N}^2\rangle$ term may be split in different ways between the mean field and the pairing field. The following prescription was used here:

$$h \rightarrow h - \lambda_2(1-2\rho), \quad \Delta \rightarrow \Delta - 2\lambda_2\kappa, \tag{1}$$

which is particularly stable numerically. In this equation, ρ is the one-body density and κ the pairing tensor.

The quasiparticle energies are perturbed by terms of the order of λ_2 times a factor lower than 1. The order of mag-

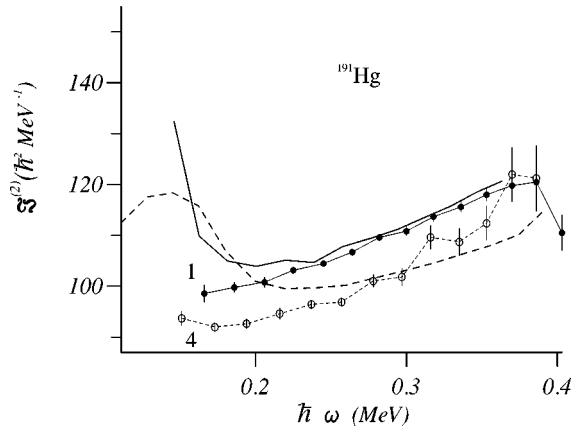

FIG. 3. Comparison between the $\mathcal{J}^{(2)}$ moments of inertia measured for bands 1 and 4 in ^{191}Hg [20] and those calculated for the one-quasiparticle excitations based on the favored (full line) and unfavored (dashed line) signatures of the $j_{15/2}$ orbital.

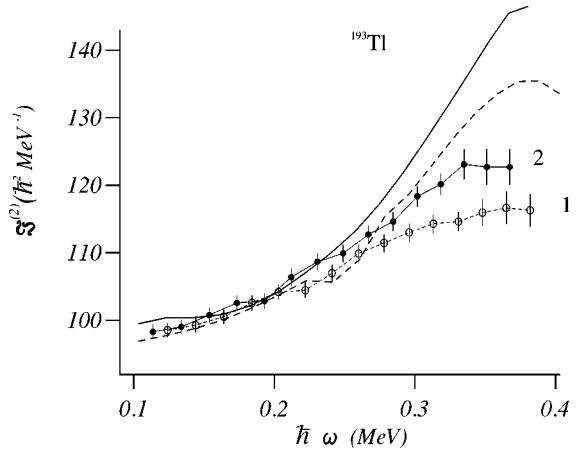

FIG. 4. Calculated dynamic moments of inertia as a function of frequency for the one-quasiparticle $i_{13/2}$ proton excitations in ^{193}Tl compared to the data for bands 1 and 2 in this nucleus [21].

nitude of λ_2 is between 100 and 300 keV. These terms are rather small, but they are state dependent. As a result, the excitation energies of two-quasiparticle excited states can in principle not be derived from unperturbed quasiparticle energies. On the other hand, the excitation energies in odd and odd-odd nuclei are obtained from differences between quasiparticle energies. This leads to the near cancellation of the terms introduced by the Lipkin-Nogami prescription. Hence, taking these reservations into account, the results shown in Table I can still be taken as fairly accurate estimates of the location of the one- and two-quasiparticle states in the odd and odd-odd isotopes under discussion.

The most recent experimental data on SD bands based on intruder $j_{15/2}$ neutrons and/or $i_{13/2}$ protons can be found in [20] for ^{191}Hg, in [21] for ^{193}Tl, and [22] for ^{192}Tl. The assignment of a specific intruder quasiparticle excitation to a band seen in an experiment relies primarily on the behavior of the dynamical moment of inertia as a function of the rotational frequency [23]. Indeed, it is expected [2] (i) that the population of intruder states will lead to a larger decrease of pairing correlations than is the case when only normal parity orbitals are involved and (ii) that this will result in a flatter moment of inertia.

Figure 3 compares the $\mathcal{J}^{(2)}$ moments for bands 1 and 4 of ^{191}Hg with the calculations for one-quasiparticle configurations based on the two signatures of the $j_{15/2}$ orbital. The general trend with frequency seen in the data is well reproduced; i.e., the unfavored signature partner has a lower $\mathcal{J}^{(2)}$ moment than the favored one. The agreement with the data is destroyed at the lowest frequencies by a neutron quasiparticle crossing. The unfavored, positive signature band is also calculated to be located $\sim$300 keV above its partner (Table I). This feature may account for the experimental observation that the latter band is fed with an intensity which is only 10% that of the $j_{15/2}$ favored partner.

As can be seen in Table I, the unfavored $i_{13/2}$ one-quasiparticle proton excitation in ^{193}Tl is calculated to be at essentially the same excitation energy as its signature partner, in agreement with the experimental observations that (i) the transition energies in band 1 are intermediate to the energies in band 2 over a large range in frequency, that (ii) levels in the two bands are linked by M1 transitions, and that (iii) the two bands are fed with approximately the same γ-ray intensity. The calculated $\mathcal{J}^{(2)}$ moments reproduce the general trend with $\hbar\omega$ very well, including the presence of a small degree of signature splitting at the higher frequencies (Fig. 4.). The more pronounced rise in the $\mathcal{J}^{(2)}$ moment seen in this nucleus, when compared to ^{191}Hg, is related to the pairing correlations which are larger for neutrons than for protons. In particular, the $j_{15/2}$ neutrons are active in this case.

Bands A and B in ^{192}Tl have been proposed as signature partner bands for reasons identical to those just described for ^{193}Tl. However, in this case the $\mathcal{J}^{(2)}$ moments of inertia were found to exhibit little variation with $\hbar\omega$. As can be seen in Fig. 5 and Table I, the calculations reproduce the data very well for the two-quasiparticle configurations where the favored signature of the $j_{15/2}$ neutron orbital is coupled to the two signatures of the $i_{13/2}$ proton orbital. Not only are the variations of the $\mathcal{J}^{(2)}$ moments with frequency small, but the difference between the values of the moments for the two signature partners is reproduced as well. The rise of the $\mathcal{J}^{(2)}$ moment at the lowest frequencies is due to the same neutron quasiparticle crossing as in ^{191}Hg.

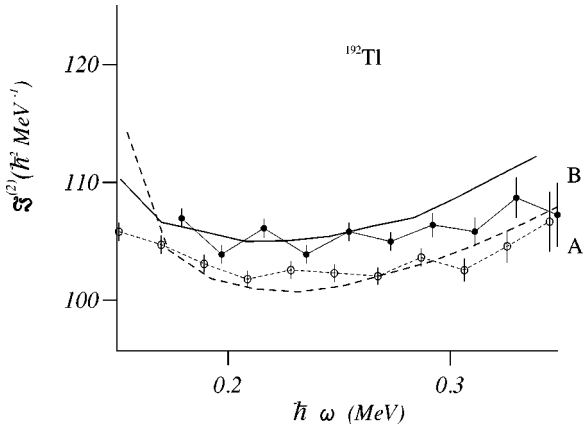

FIG. 5. $\mathcal{J}^{(2)}$ moments of inertia as a function of frequency for bands A and B of ^{192}Tl [22] compared with calculations where the favored $j_{15/2}$ neutron quasiparticle is coupled to the two signatures of the $i_{13/2}$ proton orbital.

TABLE II. Electric quadrupole moments of zero-, one- and two-quasiparticle bands (units: eb). The calculated values are taken at $\hbar\omega=0.3$ MeV. The latest published data are given for comparison. As most of these data have been obtained with the DSAM technique (except those of Ref. [30]), a 15% systematic error due to uncertainties in the calculation of the stopping powers should be added to the statistical errors quoted in the table.

	qp	$Q_{\rm calc}$	$Q_{\rm expt}$	Ref.
^{190}Hg		18.4	$17.7(^{1.0}_{1.2})$	[27]
^{191}Hg	7^-	18.0	$18(\pm 3)$	[28]
	7^+	18.0		
^{192}Hg		18.6	$17.7(\pm 0.8)$	[29]
	[642]3/2 [512]5/2	18.3	$19.5(\pm 1.5)$	[13]
	[642]3/2 7^-	18.0		
	7^+ 7^-	17.9		
^{194}Hg		18.6	$17.7(\pm 0.4)$	[29]
^{192}Tl	7^- 6^+	18.5		
	7^- 6^-	18.6		
	7^+ 6^-	19.0		
^{193}Tl	6^-	19.5		
	6^+	19.1		
^{194}Pb		20.0	$18.8(\pm 1.1)$	[30]
^{196}Pb		19.7	$18.3(\pm 3.0)$	[31]

The quadrupole moments calculated at $\hbar\omega=0.3$ MeV are compared in Table II with experimental data, when the latter are available. For the sake of completeness, moments of other nuclei (^{190,194}Hg, ^{194,196}Pb) calculated within the same framework with the same interactions have been added to Table II. As can be seen from the table, the agreement between experiment and theory is satisfactory, especially when one considers that the errors quoted in Table II are due to statistics only; i.e., an additional systematic error ($\sim$15%) should be added to most measured moments because of uncertainties in the calculation of the stopping powers inherent to the experimental technique, i.e., the Doppler shift attenuation method (DSAM) technique.

In general the changes in the calculated quadrupole moments with respect to ^{192}Hg are rather small. Furthermore, the same orbital leads to a change of the same order of magnitude in different nuclei. Recently, it has been proposed that quadrupole moments of SD bands in nuclei of the $A\sim 150$ region can be computed from the individual contributions of orbitals (additivity principle) calculated with reference to ^{152}Dy [24]. The calculations are supported by the latest data on moments for SD bands in Gd and Dy isotopes [25,26]. At first sight, this principle may appear to work also for the nuclei investigated here. For instance, the calculated change in the quadrupole moment (of 1.4 e b) between the ^{192}Hg and ^{194}Pb yrast SD configurations is the sum of increments from ^{192}Hg to the two $i_{13/2}$ configurations in ^{193}Tl (0.9 and 0.5 e b, respectively). However, there appears to be no general additivity rule in the $A\sim 190$ region. For example, the two-quasiparticle configurations involving the favored signature of the $j_{15/2}$ neutron orbital with either of the two signatures of the $i_{13/2}$ proton orbital in ^{192}Tl have the same deformation (close to that of ^{192}Hg), although the one-quasiparticle proton orbitals lead to large differences in ^{193}Tl. Clearly, the situation is more complicated than in SD bands near $A\sim 150$. Pairing plays a much larger role in the $A\sim 190$ region and this affects the quadrupole moments as well.

To complete the comparison between theoretical and experimental moments of inertia, γ-ray transition energies have also been computed. To this end, the effect on the angular momentum of the K value of the bands has been properly taken into account. The resulting γ-ray energies come within 5 keV of the experimental transitions for both bands in ^{193}Tl. In this case, the calculations confirm the spin assignments to the bands proposed in Ref. [21] on the basis of the usual fit of an Harris expansion to the $\mathcal{J}^{(2)}(\hbar\omega)$ data. The agreement between the calculations for the $j_{15/2}$ one-quasiparticle configurations and the data for bands 1 and 4 in ^{191}Hg is of the same quality at least for the transitions with $\hbar\omega>0.23$ MeV. At the lowest frequencies, the neutron quasiparticle crossing alluded to above results in larger deviations between the data and the calculations. The lowest experimental transition (280.9 keV) in band 4 is calculated to link states with spins 33/2 and 29/2, while the 310.9 keV γ ray at the bottom of band 1 is predicted to correspond to the 39/2$\rightarrow$35/2 transition. These values are 2 units larger than those deduced in Ref. [20] from the measured intensity profiles for the decay out of the SD bands and the decay into the yrast states. In the case of ^{192}Tl, the agreement between theory and experiment is similar to that achieved in ^{193}Tl only for the transition energies. Again, the calculations suggest that the spins deduced from the experimental data in Ref. [22] have to be increased by 2 units in both bands.

Taking the experimental data on the ^{192}Hg yrast SD band as a reference, Fischer *et al.* [22] showed that the alignments of bands A and B in ^{192}Tl correspond with great accuracy to the sum of the alignments of the favored $j_{15/2}$ band (band 1) in ^{191}Hg and the two $i_{13/2}$ signature partner excitations (bands 1 and 2) in ^{193}Tl. This is shown in the left panel of Fig. 6. It was concluded from this exercise that the concept of alignment additivity may be applicable to SD bands in the $A=190$ region. The alignments calculated with the present approach for the same bands are presented in the right-hand panel of Fig. 6. Since self-consistency effects due to the creation of quasiparticles are taken into account, this approach is equivalent to that adopted in the analysis of the experimental data. The trends with frequency exhibited by the alignments follow closely those seen in the data. The difference of 2 units between experiment and theory for the alignments in ^{191}Hg and ^{192}Tl reflects the $2\hbar$ difference between calculated and assigned spins discussed above. In Fig. 6, the alignments calculated for ^{192}Tl from the sum of the ^{191}Hg and ^{193}Tl contributions are also given. They follow the same trend with frequency as the ones calculated directly, but are $(1-2)\hbar$ higher. Thus, in the calculation, the additivity rule does not apply with the same degree of accuracy than seen in the data. A calculation of the alignments directly from the creation of quasiparticles appropriate for the ^{191}Hg and ^{192,193}Tl excitations on the ^{192}Hg yrast SD vacuum (an approach often followed in cranking calculations [32], and similar to that used above to obtain the energies presented in the last column of Table I) does not result in a satisfactory agreement with the data. This finding illustrates that self-consistency may restore, at least partially, additivity.

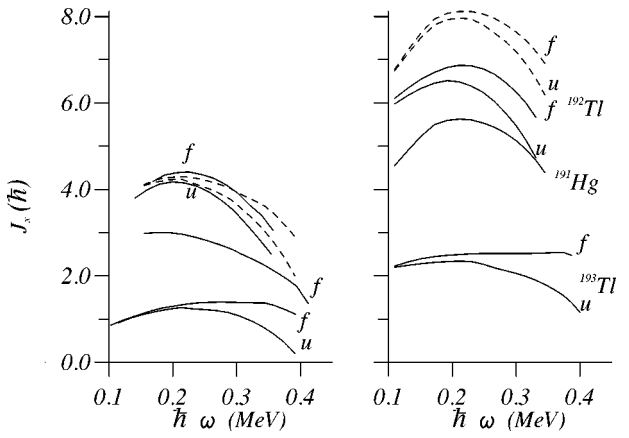

FIG. 6. Comparison between experimental (left-hand panel) and calculated (right-hand panel) alignments for the favored $j_{15/2}$ neutron excitation (band 1) in ^{191}Hg, the two signatures of the $i_{13/2}$ proton excitation (bands 1 and 2) in ^{193}Tl, and the favored $j_{15/2}$ neutron quasiparticle coupled to the two signatures of the $i_{13/2}$ proton orbital in ^{192}Tl (bands *A* and *B*). The figure also presents the test of the additivity of alignments where the alignments in ^{192}Tl are computed from the contributions in ^{191}Hg and ^{193}Tl. This test is performed for the experimental data as well as for the calculations and is shown by the dashed lines. The left-hand panel with the experimental data is taken from Ref. [22].

IV. CONCLUSIONS

In this paper, SD bands based on quasiparticle excitations created in the ^{192}Hg vacuum have been studied using the cranked HFB method with the Lipkin-Nogami prescription, the Skm* interaction, and a surface-delta, density-dependent pairing force. This method, which had earlier been found to be successful in the description of selected SD bands in the $A\sim150$ and $A\sim190$ mass regions, has been shown here to provide a satisfactory understanding of the main features of experimental data in ^{191,192}Hg and ^{192,193}Tl.

In this method, quasiparticle excitations, which are treated fully self-consistently, affect significantly the vacuum on which they are created. As a result, simple predictions of the $\mathcal{J}^{(2)}$ moments of inertia based solely on the ^{192}Hg yrast band are found to be inaccurate. In particular, the upbends and backbends seen in the excited SD bands of ^{192}Hg would not appear in our calculations without full self-consistency. These calculations are also needed for accurate predictions of the other quantities examined here such as the quasiparticle energies, the quadrupole moments and the alignments.

The present work shows a clear need for progress into two directions. The discussions above illustrate the difficulty to reproduce systematically the properties of SD bands starting from effective interactions which have not been specifically designed for this purpose. In particular, quasiparticle crossings are too sensitive to small shifts of level energies and may lead to crossing frequencies which are rather far away from the experimental observations and/or to peaks in the dynamical moment of inertia which are not present in the data. This great sensitivity provides the opportunity to improve the adjustments of Skyrme interactions. For example, the time odd terms generated by the breaking of time reversal invariance are not constrained by the data used to fit the force. As was shown in the quasiparticle diagrams, these terms can have a large impact on the excitation energy of the states, even in the absence of rotation. Comparisons between data and calculations should help in the tuning of the interaction. On the experimental side, the firm assignment of spins and parities to the SD levels as well as the determination of the excitation energy for as many SD bands as possible is needed to distinguish readily between possible configuration assignments.

ACKNOWLEDGMENTS

The authors thank M. Carpenter for valuable discussions and a careful reading of the manuscript. This work was supported by the U.S. Department of Energy under Contract No. W-31-109-ENG-38, by the ARC Convention 93/98-166 of the Belgian SSTC, and by NATO travel Grant No. CRG 97196.

[1] B. Gall, P. Bonche, J. Dobaczewski, H. Flocard, and P.-H. Heenen, Z. Phys. A **348**, 183 (1994).
[2] J. Terasaki, P.-H. Heenen, P. Bonche, J. Dobaczewski, and H. Flocard, Nucl. Phys. **A593**, 1 (1995).
[3] P. Bonche, H. Flocard, and P.-H. Heenen, Nucl. Phys. **A598**, 169 (1996).
[4] H. J. Lipkin, Ann. Phys. (N.Y.) **9**, 272 (1960).
[5] Y. Nogami, Phys. Rev. **134**, 313 (1964).
[6] H. C. Pradhan, Y. Nogami, and J. Law, Nucl. Phys. **A201**, 357 (1973).
[7] J. Bartel, P. Quentin, M. Brack, C. Guet, and H. B. Hàkansson, Nucl. Phys. **A386**, 79 (1982).
[8] P.-H. Heenen, P. Bonche, and H. Flocard, Nucl. Phys. **A588**, 490 (1995).
[9] J. Terasaki, P.-H. Heenen, P. Bonche, and H. Flocard, Phys. Rev. C **55**, 1231 (1997).
[10] T. Nakatsukasa, K. Matsuyanagi, S. Mizutori, and Y. R. Shimizu, Phys. Rev. C **53**, 2213 (1996).
[11] P.-H. Heenen *et al.* (unpublished).
[12] P. Fallon *et al.*, Phys. Rev. C **51**, 1609 (1995).
[13] A. Korichi *et al.*, Phys. Lett. B **345**, 403 (1995).
[14] B. Crowell *et al.*, Phys. Lett. B **333**, 320 (1994).
[15] M. Meyer, N. Redon, P. Quentin, and J. Libert, Phys. Rev. C **45**, 233 (1992).
[16] Y. Engel, D. M. Brink, K. Goeke, S. J. Krieger, and D. Vautherin, Nucl. Phys. **A249**, 215 (1975).
[17] P. Bonche, H. Flocard, and P.-H. Heenen, Nucl. Phys. **A467**, 115 (1987).
[18] J. Dobaczewski and J. Dudek, Phys. Rev. C **52**, 1827 (1995).
[19] B. Q. Chen, P.-H. Heenen, P. Bonche, M. S. Weiss, and H. Flocard, Phys. Rev. C **46**, 1582 (1992).
[20] M. P. Carpenter *et al.*, Phys. Rev. C **51**, 2400 (1995).
[21] S. Bouneau *et al.*, Phys. Rev. C **53**, R9 (1996).
[22] S. M. Fischer *et al.*, Phys. Rev. C **53**, 2126 (1996).

[23] W. Satula, S. Cwiok, W. Nazarewicz, R. Wyss, and A. Johnson, Nucl. Phys. **A529**, 289 (1991).
[24] W. Satula, J. Dobaczewski, J. Dudek, and W. Nazarewicz, Phys. Rev. Lett. **77**, 5182 (1996).
[25] H. Savajols *et al.*, Phys. Rev. Lett. **76**, 4480 (1996).
[26] D. Nisius *et al.*, Phys. Lett. B **380**, 18 (1997).
[27] H. Amro *et al.*, Phys. Lett. B **413,** 15 (1997).
[28] M. P. Carpenter *et al.*, Phys. Lett. B **240**, 44 (1991).
[29] E. F. Moore *et al.*, Phys. Rev. C **55**, 2150 (1997).
[30] R. Krucken *et al.*, Phys. Rev. C **55**, R1625 (1997).
[31] E. F. Moore *et al.*, Phys. Rev. C **48**, 2261 (1993).
[32] R. Bengtsson and S. Frauendorf, Nucl. Phys. **A327**, 139 (1979).